Hindawi
Geofluids
Volume 2021, Article ID 9953498, 17 pages
https://doi.org/10.1155/2021/9953498

Research Article

Experimental Investigations of Offshore Sand Production Monitoring Based on the Analysis of Vibration in Response to Weak Shocks

Yichen Li,[1] Gang Liu,[1] Zongwen Jia,[2] Min Qin,[3,4] Gang Wang,[1] Yinan Hu,[1] Jialin He,[5] and Kai Wang[1]

[1]*School of Petroleum Engineering, China University of Petroleum (East China), Qingdao 266580, China*
[2]*Drilling and Production Research Department, CNOOC Research Institute Co., Ltd., Beijing 100089, China*
[3]*School of Civil Engineering and Architecture, Southwest University of Science and Technology, Mianyang 621002, China*
[4]*Shock and Vibration of Engineering Materials and Structures Key Laboratory of Sichuan Province, Southwest University of Science and Technology, Mianyang 621002, China*
[5]*National Nuclear Security Technology Center, Beijing 102401, China*

Correspondence should be addressed to Gang Liu; lg_communication@126.com

Received 8 March 2021; Accepted 30 June 2021; Published 29 July 2021

Academic Editor: Tianran Ma

Sand production is a problem that is often encountered in unconventional oil and gas exploitation and that is difficult to effectively solve. Accurate online monitoring of sand production is one of the keys to ensuring the safety and long-term production of oil wells as well as efficient production throughout the life cycle of production wells. This paper proposes a method for monitoring sand production in offshore oil wells that is based on the vibration response characteristics of sand-carrying fluid flow impinging on the pipe wall. This method uses acceleration sensors to obtain the weak vibration response characteristics of sand particles impinging on the pipe wall on a two-dimensional time-frequency plane. The time-frequency parameters are further optimized, and the ability to identify weakly excited vibration signals of sand particles in the fluid stream is enhanced. The difference between the impact response of the sand particles and the impact response of the fluid flow to the pipe wall is identified, and corresponding indoor verification experiments are carried out. Under different sand contents, particle sizes, and flow rates (sand content 0-2‰, sand particle size 96-212 μm, and flow velocity 1-3 m/s), the impact response frequency of sand particles to the pipe wall exhibits good consistency. The characteristic frequency band of sand impacting the pipe wall is 30-50 kHz. A statistical method is used to establish the response law of the noise signal of the fluid. Based on this knowledge, a real-time calculation model of sand production in offshore oil wells is constructed, and the effectiveness of this model is verified. Finally, a field test is carried out with a self-developed sand production signal dynamic time-frequency response software system on 4 wells of an oil production platform in the Bohai Sea. This system can effectively distinguish sand-producing wells from non-sand-producing wells. The dynamic time-frequency response, field test results, and actual laboratory results are consistent, verifying the effectiveness of the method proposed in this paper and further providing a theory for improving the effectiveness of the sand production monitoring method under complex multiphase flow conditions. This study also provides technical guidance for the industrial application of sand production monitoring devices in offshore oil wells.

1. Introduction

Unconventional oil and gas fields are currently a focus of oil and gas exploration and development in the petroleum industry. Due to the poor reservoir properties and fluid flow capacity of tight sandstone, hydraulic fracturing technology has been widely used in the development of tight oil reservoirs. With the exploitation of oil reservoirs, the rock structure of the reservoir becomes destroyed [1, 2], causing sand particles to separate from the rock mass. The fluid is then

carried into the wellbore or production pipeline. Sand production in oil wells is one of the key problems that plague the safety and efficiency of oil fields. Excessive sand production will cause problems such as wear of the downhole and surface facilities, sand burial in the pay zone, and the reduction in or halting of oil and gas well production [3]. Therefore, effective sand production monitoring technology is key for ensuring oil well safety and long-term production [4–6]. Through the research and application of online monitoring systems for sand production in production wells, real-time information on sand production in oil wells can be continuously and effectively obtained. These data can be used to guide the formulation of moderate sand production strategies and sand control plans for sand production wells and to provide real-time data for informing intelligent oilfield production management. This approach extends the life of oil wells, improves the production efficiency of oil wells, and extends the economic development cycle of oil fields.

Sand production monitoring methods can be divided into two types: nonimplanted monitoring methods and implanted monitoring methods [7]. Implanted monitoring methods involve installing a probe inside the pipeline to sense the impact of sand particles on the sensitive components. This approach is suitable for a single low-velocity fluid carrying sand [8, 9]. Kesana et al. [10] used electrical resistance (ER) probes to study the effects of particle size and fluid viscosity on annulus flow and slug flow. However, this method requires changing the production pipeline during installation and has problems such as a short service life, signal attenuation, and a low accuracy. Therefore, nonimplanted monitoring methods are generally used to obtain sand production information. These methods involve installing sensors on the outer wall of the pipeline to sense the impact of sand particles on the pipeline and identify the sand production information of oil wells by analyzing the vibration signal characteristics of the sand-carrying fluid flow [11]. Hii et al. [12] successfully obtained the characteristics of the solid content in a gas-solid two-phase flow based on the principle of acoustic emission. El-Alej et al. [13] obtained the characteristics of the sand content in a water-sand two-phase flow using acoustic emission technology. Sampson et al. [14] established a mathematical model of sand production in oil wells based on acoustic measurements. Ibrahim and Haugsdal [15] further considered the influence of noise signals induced by oil flow on the sand production model. Gao et al. [16] proposed reducing the mathematical model of sand production after considering the noise signals induced by oil flow. The existing sand detection methods have practical advantages in the recognition of solid particles in a wide frequency range and at higher speeds. However, the key predictive information is contained in the weak excitation signal of the particles impacting the tube wall. Therefore, it is very important to enhance the recognition ability of weakly excited vibration signals of sand particles in a fluid stream.

At present, the main difficulties in the identification of oil well sand production signals and the monitoring of oil well sand production volumes include the following: (1) the sand production signal is very weak compared to the high-intensity fluid flow and strong noise signals, but it contains sand production information. The effective signal is often lost in this background noise, so a short-time Fourier transform (STFT) can be applied to effectively distinguish the signals of the sand impacting the pipe wall from those of the fluid flow impacting the pipe wall in the frequency domain to make it easier to recognize the weakly excited vibration of sand in the fluid flow signal. (2) Further clarification of the relationship between the sand production signal and the sand production parameters is needed to obtain a more accurate sand content calculation model. The power spectral density is used to characterize the relationship, which can characterize the distribution of the time domain signal with frequency [17]. (3) Based on the vibration signal characteristics of the sand-carrying fluid flow, a sand production monitoring software system with multiwell real-time monitoring and sand content identification functions must be compiled.

This paper proposes an oil well sand production monitoring method based on a characteristic analysis of the vibration signal of sand-carrying fluid flow impacting a pipe wall. In this paper, a high-frequency acceleration sensor is used to experimentally study the difference between the vibration response characteristics of the sand particles impacting the pipe wall and the fluid impacting the pipe wall. Through the time-frequency joint analysis method, the recognition ability of the weak excitation signal of the sand particles within the strong noise signal of the fluid flow is improved. On this basis, the characteristic frequency of sand impacting the pipe wall is discussed. A statistical method is used to establish the response law of the noise signal of the fluid. Based on indoor simulation experiments, the actual oil well particle size distribution is considered. Under single-factor conditions such as the sand particle size and flow velocity, the influence of flow velocity and sand particle size on vibration energy is studied. Additionally, a sand production calculation model for oil wells is established based on several indoor simulation experiments, and the effectiveness of the model is verified. Based on this model, a set of sand production monitoring software systems with a multichannel sand production dynamic monitoring function is compiled. Field test research is carried out on 4 test wells of an oil production platform in the Bohai Sea to verify the effectiveness of the method proposed in this paper and to provide information for its use in industrial oil well sand production monitoring.

2. Methods

2.1. Principles of Sand Vibration Monitoring. Sand production is a very common phenomenon in oil wells and is difficult to avoid in the production process of sand-carrying crude oil. When sand-carrying fluid flows through a 90° elbow of a pipeline at a high speed, inertia will act on the sand particles due to the sudden change in the fluid flow direction. The constraints of the drag force of the fluid are overcome, and the particles hit the pipe wall and vibrate, as shown in Figure 1. The sand particles produce a certain impact kinetic energy (KE) due to the work done on the pipe wall. The sensor on the outside of the elbow picks up the vibration characteristics and further converts them into the required

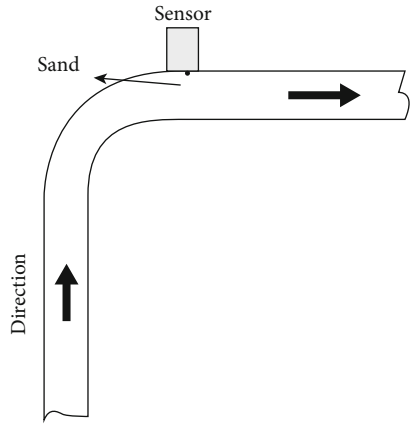

Figure 1: Principles of sand vibration monitoring.

sand particle parameters. The KE generated by the sand particles is given in the following equation:

$$\mathrm{KE} = \frac{mv^2}{2}, \tag{1}$$

where m is the mass of sand grains and v is the velocity of the particles hitting the pipe wall. This article assumes that the particles are standard spherical particles and does not consider the impact of particle shape on impact force. Equation (1) shows that the KE of the sand grains is proportional to the mass of the sand grains and has a parabolic growth relationship with the fluid velocity. For low-viscosity dilute particulate flow, the interactions between particles and viscous force are not considered.

2.2. Recognition and Extraction of Sand Grain Characteristics in Fluid Flow Vibration Signals. The vibration signal generated by the sand-carrying fluid flow impacting the pipe wall is from the vibrations generated under the excitation of random force and can be regarded as a nonstationary vibration signal. The time-frequency analysis method is a powerful tool for analyzing nonstationary signals. The vibration signal of low-content sand particles impacting the pipe wall in the fluid flow is very weak. To effectively distinguish the sand particle impact signal and the fluid flow impacting the pipe wall signal in the frequency domain, it is necessary to account for the fact that the signal characteristics cannot be characterized in the frequency domain. The signal is processed and identified by a time-frequency analysis method based on the STFT.

The STFT is obtained by sliding a fixed-width time window along the time axis to divide the signal into multiple equal periods. Within a short period of time, the signal is considered stable, and the Fourier transform is used to obtain the spectral information of the signal. This method comprehensively considers the spectral information of all time periods to obtain a two-dimensional time-frequency analysis result. The STFT of the discrete signal can be expressed by Equation (2) [18].

$$\mathrm{STFT}^k(f) = \sum_{i=1}^{n} x_k(i) w(i) e^{-j2\pi nf}, \tag{2}$$

where $w(i)$ is the window function and the width of the window is equal to the signal segment when the stationary assumption is established.

The power spectrum of the vibration signal generated by the sand-carrying fluid stream impacting the pipe wall reflects the change in the signal power, with the frequency in the unit frequency band. Therefore, the energy of the random signal can be obtained with the frequency change by the power spectral density function [19]. When using the STFT for frequency domain signal analysis, the power spectral density function is commonly used to characterize the signal and is expressed as

$$P_{xx}^h(f) = \frac{1}{\sum_{i=1}^{n} w^2(i)} \left[\sum_{i=1}^{n} x_h(i) w(i) e^{-j2\pi nf} \right]^2. \tag{3}$$

Shi et al. [20] used the STFT to process the Doppler frequency shift signal and revealed the correlation between the time-varying velocity characteristics of the flow field and the flow field structure. Tang et al. [21] used the STFT to analyze the signal obtained by a hydrophone and obtained the time interval of a certain bubble condensation process. Sheikhi et al. [22] used the power spectrum of the vibration signal to better predict the main hydrodynamic characteristics of a liquid-solid fluidized bed. Khan et al. [23] used the STFT to determine the size of bubbles obtained by computational fluid dynamics (CFD) simulation. Wang et al. [24, 25] analyzed different multiphase flow fluid properties and the characteristics of vibration signals excited by sand particles impacting a pipe wall in multiphase flow and applied STFT time-frequency analysis to obtain the characteristic frequency bands of the sand.

In the process of acquiring signals from the sensor, some interference and noise will inevitably be incorporated, which will affect the sand production monitoring results. Therefore, it is necessary to filter the interference noise. In the real-time signal processing of oil-water-sand multiphase flow, to ensure the stability and linear phase characteristics of the signal, a finite impulse response (FIR) digital filtering method is selected to further improve the signal-to-noise ratio. For the FIR filter, the following system function of finite length is used to express the system function of the FIR filter [26].

$$H(z) = \sum_{n=0}^{N-1} h(n) z^{-n}. \tag{4}$$

Regarding the design method, this paper adopts the Butterworth filter and the Chebyshev filter. The maximum flat amplitude characteristic in the passband of the Butterworth filter decreases monotonically with increasing frequency. The error of the Chebyshev filter is observed as equal ripples in the specified frequency band. The amplitude characteristics of the Chebyshev type I filter are observed as equal

ripples in the passband and are monotonic in the stopband. The amplitude characteristics of the Chebyshev type II filter are observed as a monotonic descent in the passband, whereas equal ripples are present in the stopband [27].

The form of the squared amplitude function of the Butterworth filter is given by

$$A\left(\Omega^2\right) = \frac{1}{1 + \left(j\Omega/j\Omega_c\right)^{2N}}, \tag{5}$$

where Ω_c is the cutoff frequency of the filter and N is the order of the filter.

The form of the amplitude-frequency characteristics of the Chebyshev filter is given by

$$H\left(\Omega^2\right) = \frac{1}{1 + \varepsilon^2 T_n^2\left(j\Omega/j\Omega_c\right)}. \tag{6}$$

In the formula, ε represents the coefficient of fluctuation, T_n represents the nth-order Chebyshev polynomial, and its form is expressed as

$$T_n(\Omega) = \begin{cases} \cos\left(n\cos^{-1}(\Omega)\right) |\Omega| \le 1, \\ \mathrm{ch}(n\mathrm{ch}(\Omega)) |\Omega| > 1. \end{cases} \tag{7}$$

3. Experimental Device and Experimental Design

3.1. Experimental Device. The indoor evaluation device for oil well sand production monitoring used in this work is a large-displacement sand production monitoring test bench based on a screw pump, which can simulate the standard sand content under different working conditions. It can be used repeatedly with a single-phase fluid or a multiphase fluid. This study provides a reliable and stable monitoring and calibration platform for the monitoring of sand-carrying fluids. The experimental device mainly includes a multiphase flow loop system and a sand production monitoring system, as shown in Figure 2. The screw pump circulates the sand-carrying fluid. The speed of the screw pump is controlled by adjusting the frequency of the inverter, thereby changing the flow rate of the fluid in the circulation pipeline. To ensure that the sand particles are fully mixed in the fluid, a stirrer is installed in the fluid storage tank to mix the sand particles and the fluid evenly. After the sand-carrying fluid flow is fully developed, it flows through the elbow equipped with the sensor and then returns to the fluid storage tank to achieve multiphase flow circulation. The test tube is made of 304 steel. The outer diameter of the pipeline is 34 mm, the inner diameter is 25 mm, and the radius of curvature of the elbow is 2.5D (where D is the nominal diameter).

The sand production monitoring data acquisition system uses the 357B03 acceleration sensor produced by the PCB company to obtain the vibration signal of the sand-carrying fluid flow impacting the pipe wall. The sensor is installed at a location 1-2 times the pipe diameter downstream of the elbow. The signal is transmitted to the acquisition card via the cable, and after being converted into a digital signal, it is collected and analyzed by sand monitoring software in the computer.

3.2. Experimental Design. The experimental conditions for studying the characteristics of the vibration signal characteristics of the sand-carrying fluid flow impacting the pipe wall under multifactor conditions, which mainly include the relationship between the characteristics of the sand production signal and the particle size distribution, the sand content, and the flow velocity, are shown in Table 1.

Experiment 1 studied the influence of different sand contents on the characteristics of the sand production monitoring signals. The sand content ranged from 0 to 0.2%, the viscosity of the sand-carrying fluid was 1 mPa·s, the fluid flow rate was 1.5 m/s, and the sand particle size was 150 μm. Experiment 2 studied the characteristics of the sand monitoring signal under different particle size conditions, with sand particle sizes of 96 μm, 125 μm, 150 μm, 180 μm, and 212 μm. The sand-carrying fluid viscosity was 1 mPa·s, and the fluid flow rate was 1.5 m/s. Experiment 3 studied the influence of different flow velocities on the characteristics of the sand production monitoring signals. The flow velocity range was 1-3 m/s, and the viscosity of the sand-carrying fluid was 1 mPa·s. To study the impact of the fluid impacting the pipe wall on the sand production background noise signal, experiments were carried out without sand and with an experimental sand sample with a particle size of 180 μm.

4. Results and Discussion

4.1. Analysis of the Signal Characteristics of Sand Production under Different Sand Content Conditions. To study the vibration signal characteristics of sand-carrying fluid impacting the pipe wall, the influence of different sand contents on the signal characteristics of sand production was first studied through experiment 1. Figure 3(a) shows the sand produced when the fluid viscosity was 1 mPa·s; the sand particle size was 150 μm; the pipeline flow rate was 1.5 m/s; and the sand contents were 0, 0.5‰, 1‰, 1.5‰, and 2‰. Figure 3(a) shows that both the signal of the impingement of the pipe wall by the sand-free stream and the signal of the impingement of the pipe wall by the sand-carrying stream had strong signal characteristics in the frequency range of 0-20 kHz. Therefore, this frequency band was the vibration signal excited by the fluid flow impacting the pipe wall, and most frequencies were mainly concentrated in the low-frequency band below 20 kHz. This frequency band is the vibration signal excited by the fluid impacting the pipe wall, and the low content of sand in the fluid flow impacts the vibration signal of the tube wall, which is very weak.

To effectively distinguish the signal of sand impacting the pipe wall and the signal of fluid flow impacting the pipe wall in the frequency domain, it is necessary to account for the fact that the signal characteristics cannot be characterized in the frequency domain. The signal was processed and identified by a time-frequency analysis method based on the STFT, and the two-dimensional time-frequency spectrum is shown in Figure 3(b). This figure clearly shows that in the

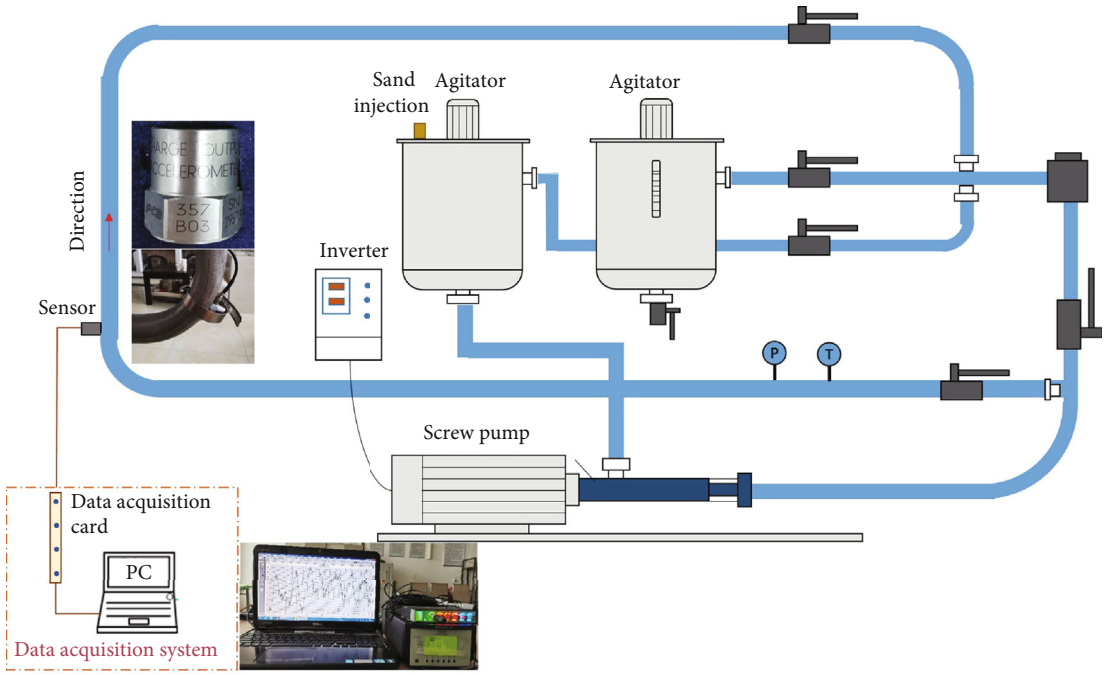

Figure 2: Schematic diagram of the experimental facility.

Table 1: Experimental parameters.

	Flow velocity (m/s)	Sand content (‰)	Sand particle size (μm)
Experiment 1	1.5	0, 0.5, 1, 1.5, 2	150
Experiment 2	1.5	0, 0.5, 1, 1.5, 2	96, 125, 150, 180, 212
Experiment 3	1, 1.5, 2, 2.5, 3	0, 0.5, 1, 1.5, 2	180

low-frequency band below 20 kHz, the vibration signals before and after the sand had relatively high-frequency characteristics, consistent with the results in Figure 3(a). In the 30-50 kHz frequency band, as the sand content increased, the relative energy of the sand vibration signal increased significantly. Therefore, this frequency band is the characteristic frequency band of the vibration signal of the sand impacting the pipe wall. Compared with Figure 3(a), the time spectrogram based on the STFT effectively compensates for the defect that the signal characteristics cannot be described in the frequency domain and enhances the recognition ability of the weakly excited vibration signal of the gravel in the fluid flow.

To reduce the impact of the strong noise signal from the signal of the fluid impacting the pipe wall, the results from the characteristic analysis of the sand measurement signal under different sand content conditions were further analyzed, and the effective frequency range of the sand vibration signal was filtered from 30 to 50 kHz. The frequency domain and time domain of the filtered monitoring signal are shown in Figures 3(c) and 3(d), respectively. Within the effective frequency range of sand production, the time domain amplitude and frequency domain amplitude of the change in the sand content increased as the sand content increased.

4.2. Characteristic Analysis of the Sand Measurement Signals under Different Particle Size Conditions. Figures 4(a) and 4(b) show the test results when the fluid had a viscosity of 1 mPa·s; a sand content of 1‰; a pipeline flow rate of 1.5 m/s; and sand grain sizes of 96 μm, 125 μm, 150 μm, 180 μm, and 212 μm. For the frequency domain diagram and time spectrum diagram of the sanding signal, the high energy intensities of the sand monitoring signal mainly concentrated in the low-frequency band below 20 kHz. The results of experiment 1 show that this frequency band corresponds to the vibration signal excited by the fluid impacting the pipe wall, as shown in Figure 4(b). Figure 4(b) also shows that as the particle size of the sand increased, the energy of the vibration signal of sand production increased.

To study the characteristics of the sand measurement signal under different particle size conditions, the effective frequency range of the sand particle vibration signal was filtered from 30 to 50 kHz. The filtered time domain diagram is shown in Figure 4(c). As the sand particle size increased, the time domain amplitude of the sand output monitoring signal clearly increased. After filtering and denoising, the power spectrum amplitude of the sand vibration signal was calculated. Under the experimental conditions of a pipeline flow rate of 1.5 m/s, the resulting power spectrum densities

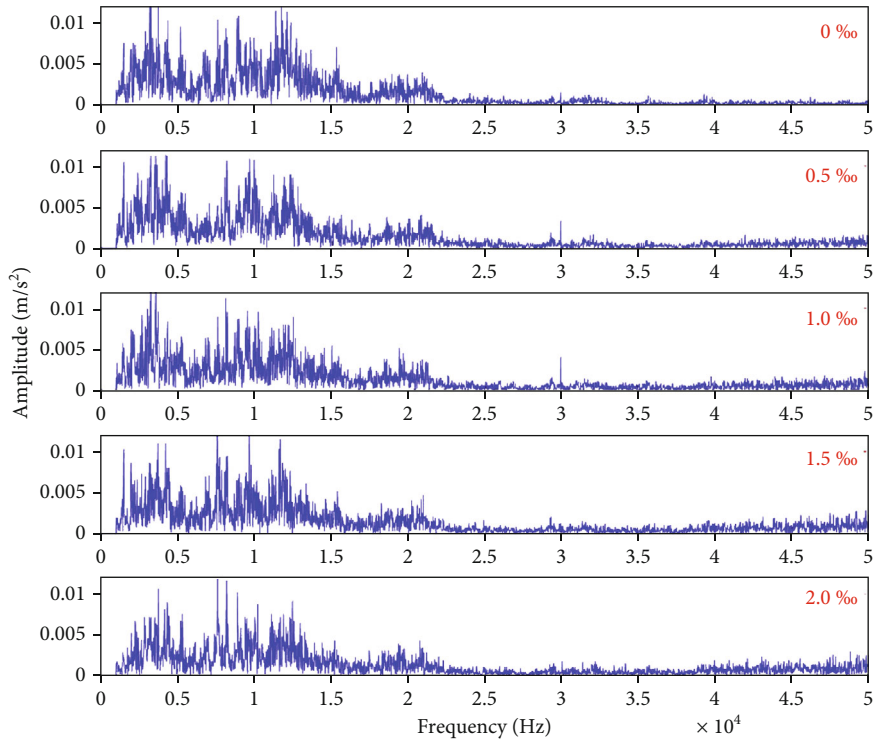

(a)

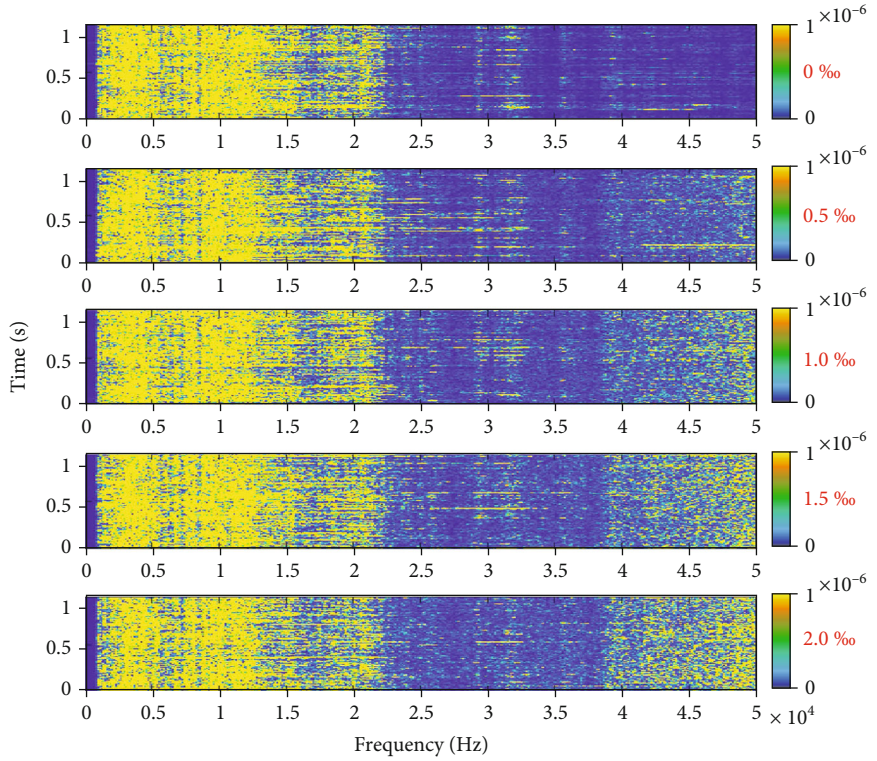

(b)

Figure 3: Continued.

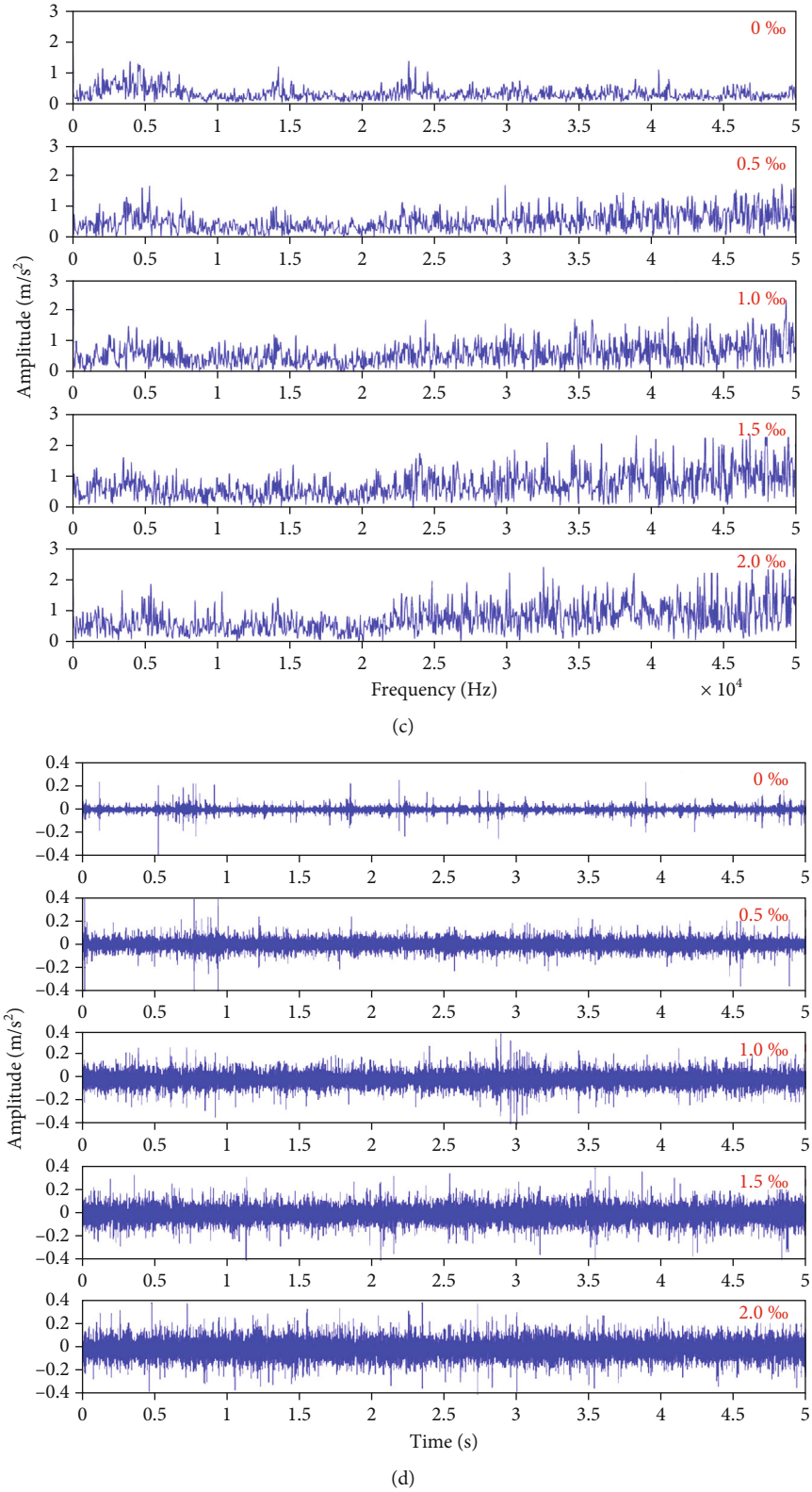

Figure 3: Characteristic analysis of the sand measurement signal under different sand content conditions (particle size 150 μm, flow velocity 1.5 m/s): (a) frequency domain diagram; (b) time spectrum; (c) 30-50 kHz frequency domain diagram; (d) 30-50 kHz time domain diagram.

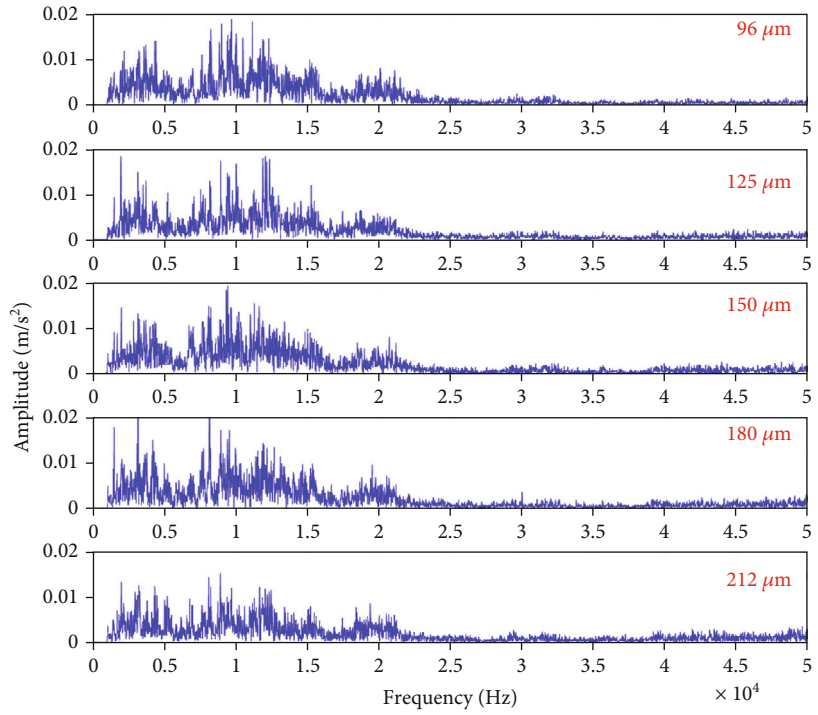

(a)

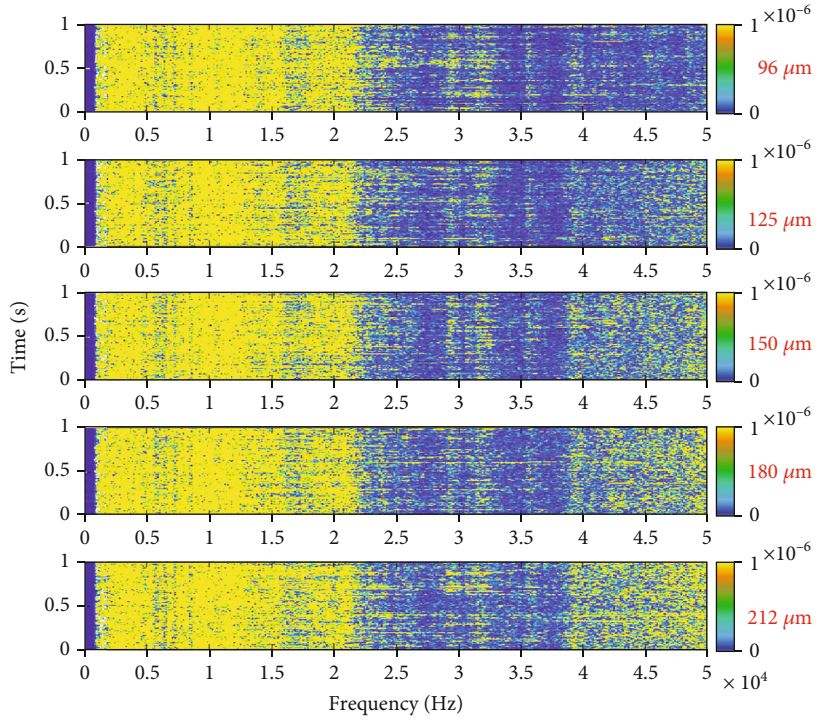

(b)

Figure 4: Continued.

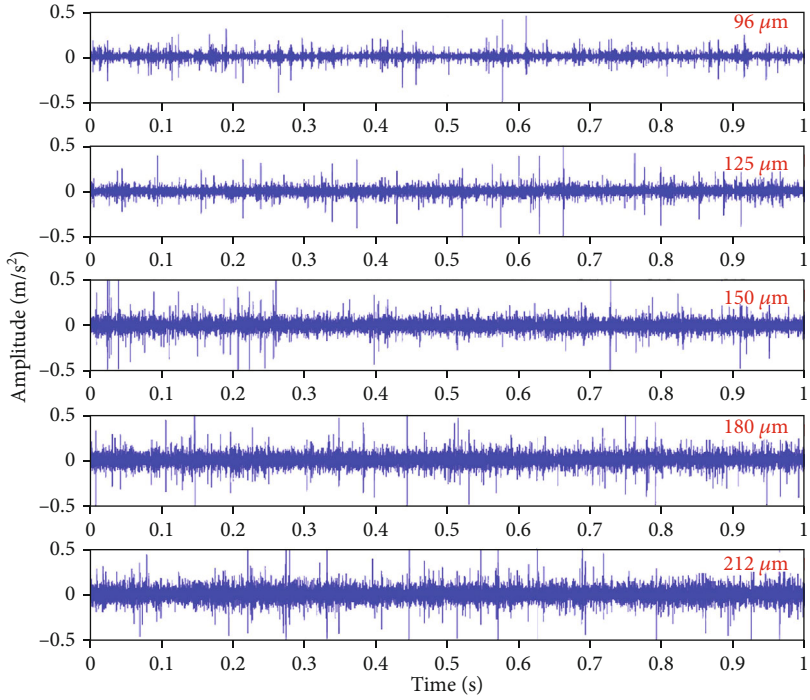

(c)

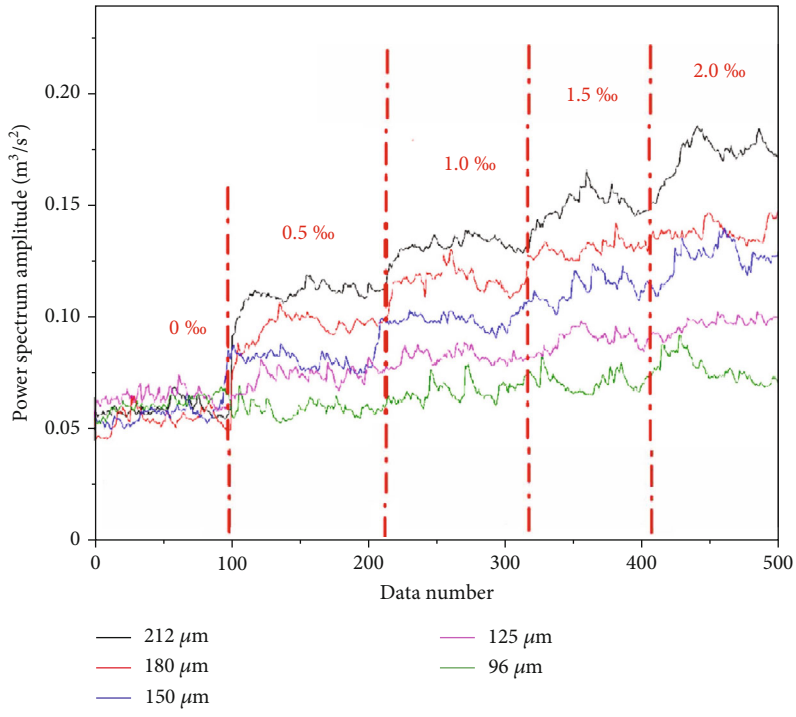

(d)

Figure 4: Analysis of the signal characteristics of sand production under different particle size conditions (sand content 1‰, flow velocity 1.5 m/s): (a) frequency domain diagram; (b) time spectrum; (c) 30-50 kHz time domain diagram; (d) power spectrum analysis.

of the sand vibration signals with different sand particle sizes are shown in Figure 4(d). This figure shows that the power spectrum density of the sand output signal increased as the sand content increased when the sand particle size and pipeline flow rate were constant; when the sand content and pipeline flow rate were constant, the sand output signal of the power spectrum increased as the sand particle size increased.

4.3. Characteristic Analysis of Sand Measurement Signals under Different Flow Velocities. To further study the influence of different flow rate conditions on the vibration

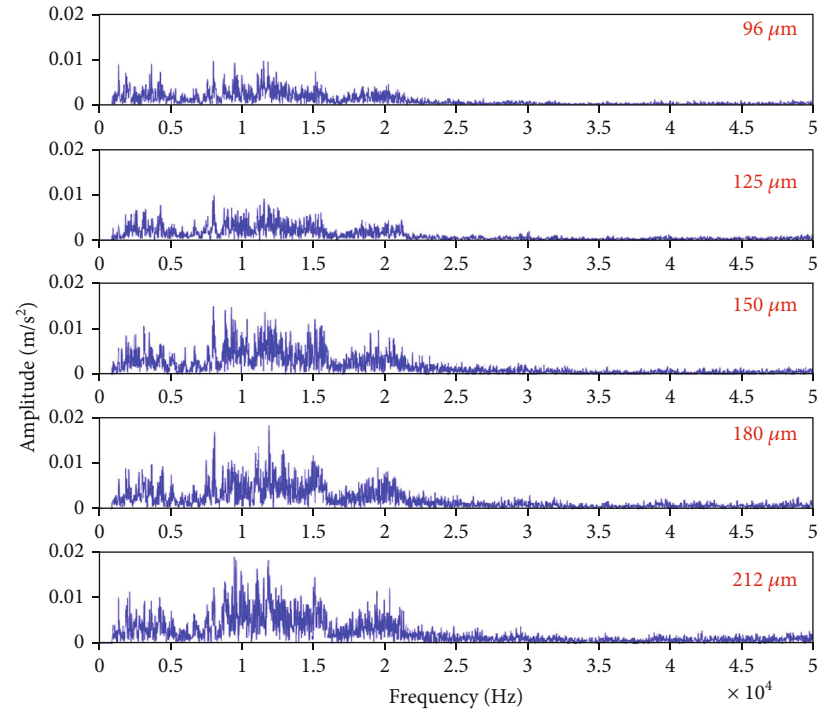

(a)

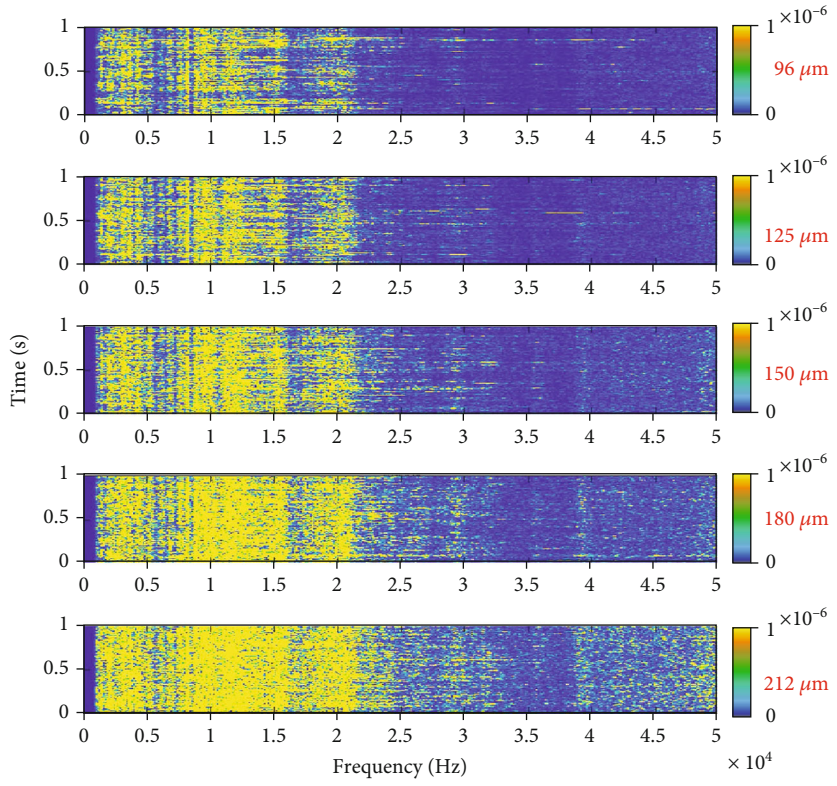

(b)

Figure 5: Continued.

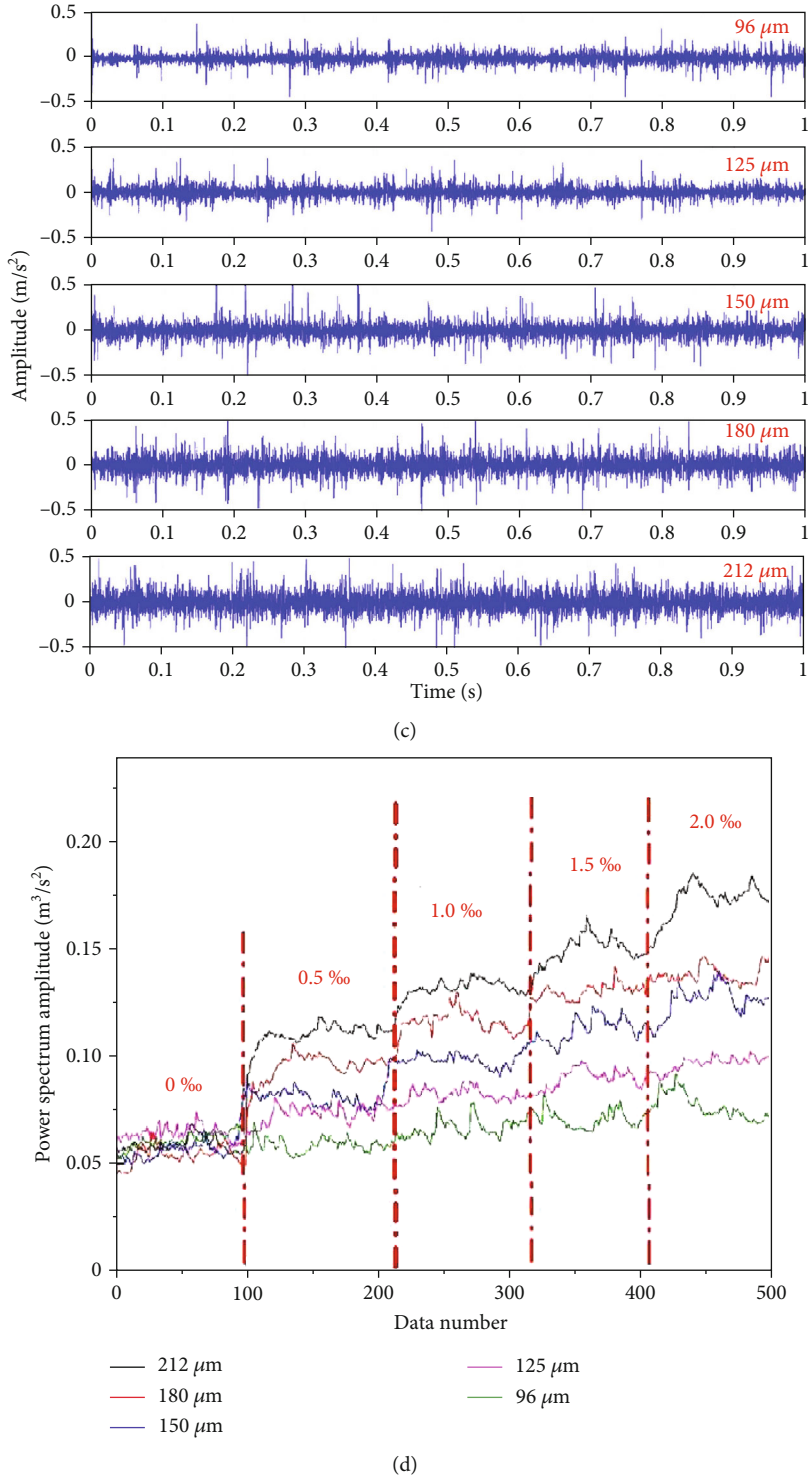

Figure 5: Characteristic analysis of the sand measurement signal under different flow velocity conditions (sand content 1‰, particle size 180 μm): (a) frequency domain diagram; (b) time spectrum; (c) 30-50 kHz time domain diagram; (d) power spectrum analysis.

signal characteristics of the sand-carrying fluid impacting the pipe wall, indoor sand production monitoring experiments were carried out at different flow velocities. Figures 5(a) and 5(b) show the sand vibration signal frequency domain graph and time-frequency domain graph results for a fluid viscosity of 1 mPa·s, a sand content of 1‰, a sand particle size of 180 μm, and pipeline flow velocities of 1 m/s, 1.5 m/s, 2 m/s, 2.5 m/s, and 3 m/s. In the figure, in the 0-20 kHz frequency band of the strong noise signal of the fluid flow, as the flow rate increased, the frequency domain amplitude and power spectrum energy of the fluid flow signal increased.

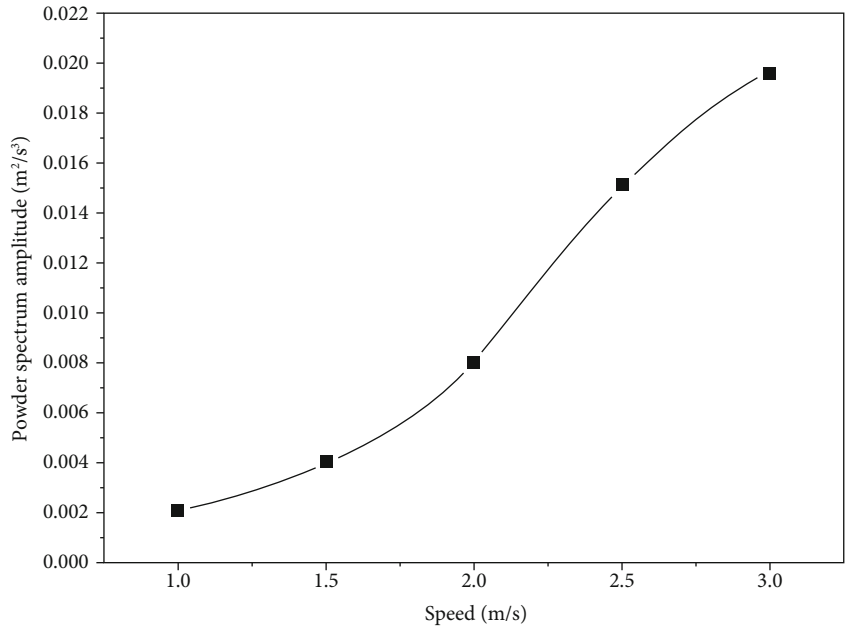

Figure 6: Vibration signal energy of fluid impacting the pipe wall.

The relationship between the pipeline flow velocity and the sand production monitoring signal under different experimental conditions was determined. According to the analysis results of the effective frequency range of the sand vibration signal, the vibration signal generated by the impact of sand particles on the pipe wall was filtered and noise-reduced in the characteristic frequency band of 30-50 kHz. A noise processing and the filtered time domain diagram of the sand production monitoring signal is shown in Figure 5(c) for each of the pipeline flow velocities tested. As the pipeline flow rate increased, the time domain amplitude of the sand production monitoring signal increased. Figure 5(d) shows the power spectrum density of the sand measurement signal when the sand particle size was 180 μm, and the pipe flow velocities were 1 m/s, 1.5 m/s, 2 m/s, 2.5 m/s, and 3 m/s. For a certain pipeline flow rate, as the sand content increased, the power spectrum amplitude of the sand output monitoring signal increased accordingly. For a certain sand content, as the flow velocity increases, the power spectrum and amplitude of the sand output monitoring signal increased accordingly.

According to the calculation results of the power spectral density, the curves of the relationships between the fluid flow noise signal and pipeline flow rate at different flow velocities were obtained, as shown in Figure 6.

4.4. Sand Production Monitoring Calculation Model. The sand monitoring signal was collected by the acceleration sensor as a charge signal, converted into a voltage signal after charge amplification and conversion, and finally converted into the relative vibration energy by a signal acquisition card and related signal processing modules. The vibration energy can describe the sand content trend, and on this basis, a mathematical model of sand mass flow can be established. To obtain the relationship between the sand production information and the sand production monitoring signals under different experimental conditions, the relative average vibration energy of the sand production vibration signal was represented by $\mathrm{VE}_{\mathrm{fluid-sand}}$.

$$\mathrm{VE}_{\mathrm{fluid-sand}} = \frac{1}{T}\int_0^T V^2(t)dt, \tag{8}$$

where $V(t)$ is the average voltage value of the signal of the sand-carrying fluid impacting the pipe wall and T is the duration of the signal sample.

The monitored vibration signal of sand production was subtracted from the average energy G_{fluid} of the vibration signal generated by the fluid with zero sand content that impacts the pipe wall under the experimental conditions to obtain the numerical noise reduction processing result of the sand production monitoring signal. A polynomial fitting method was adopted to fit the energy signal generated by the fluid impacting the tube wall. The increase in the order of the polynomial leads to an increase in the calculation error, which also affects the stability of the calculation and increases the difficulty of the calculation. Combined with the characteristics of the vibration signal generated by the fluid impacting the pipe wall, a third-order polynomial was selected. The average vibration energy generated by the impact of fluids at different flow velocities on the pipe wall in Figure 6 was fitted with the following equation:

$$G_{\mathrm{fluid}}(v) = A_{\mathrm{fluid}} \cdot v^3 + B_{\mathrm{fluid}} \cdot v^2 + C_{\mathrm{fluid}} \cdot v + D_{\mathrm{fluid}}. \tag{9}$$

The fitting coefficients are shown in Table 2.

Equation (9) can be used to calculate the fluid noise power spectrum under various flow rate conditions. To quantitatively analyze and obtain accurate sand production,

Table 2: Cubic polynomial fitting coefficients.

A_{fluid}	B_{fluid}	C_{fluid}	D_{fluid}	R-square
0.0187	-0.0341	0.00206	-0.003	0.9995

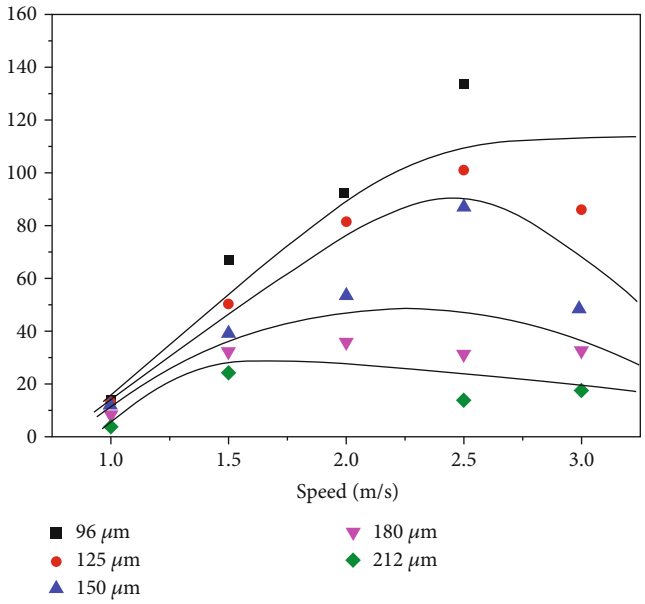

Figure 7: Correction coefficient plate.

a linear calibration coefficient, C, was introduced to construct a sand production model. Equation (10) is the basic model for calculating the amount of sand in the self-designed sand monitoring software.

$$q_{sand} = C * [VE_{fluid-sand} - G_{fluid}(v)]. \quad (10)$$

According to the analysis results of the vibration signal power spectrum obtained under different experimental conditions, the power spectrum of the noise in the fluid flow single of the corresponding flow velocity was subtracted to obtain the vibration response power spectrum of the sand particle impacting the pipe wall. On this basis, according to the relationship between the actual sand content and the calculated sand power spectrum, the parameter C was calculated. Finally, a chart of correction coefficients under different flow velocities and particle size conditions was established, as shown in Figure 7.

4.5. Field Test Verification

4.5.1. Sand Monitoring Software Compiling. According to the results from analyzing the vibration signal characteristics of the sand-carrying fluid flow under the conditions of different sand contents, particle diameters, and flow velocities and the constructed sand production model, a set of sand production monitoring systems with a multichannel sand production dynamic monitoring function was compiled and improved. Figure 8(a) shows the real-time dynamic time-frequency spectrum of the indoor monitoring experiment. The real-time sand production monitoring module includes functions for the input of the production well information, reduction in the fluid noise, and calculation of the sand production and cumulative sand production, which allow multichannel output online sand monitoring, as shown in Figure 8(b).

4.5.2. Field Application of Sand Production Monitoring Based on a Characteristic Analysis of the Vibration Signal of Sand-Carrying Fluid Flow. To verify the reliability of the sand production monitoring method based on the analysis of the vibration signal characteristics of the sand-carrying fluid flow under the on-site production conditions and application environment, a multichannel sand production monitoring system was used to conduct on-site sand production monitoring tests on four wells of an offshore mining platform. The wellheads monitored by channels AD0, AD1, AD2, and AD3 corresponded to velocities of 0.30 m/s, 0.87 m/s, 2.29 m/s, and 2.22 m/s and moisture contents of 41%, 92.1%, 91%, and 91.7%, respectively. The real-time monitoring frequency domain diagram and time-frequency spectrum of each wellhead are shown in Figures 9(a) and 9(b), respectively.

The frequency domain spectrum in Figure 9(a) shows that the real-time monitoring spectrum of the two wells monitored by channels AD0 and AD1 has a dynamic response in the characteristic frequency band of the sand production vibration signal. The two wells monitored by channels AD2 and AD3 do not exhibit an obvious dynamic response to sand impacting the pipe wall. In Figure 9(b), the blue line in the time domain diagram is the original vibration signal, and the red line is the vibration signal after filtering the characteristic frequency bands of the sand impacting the pipe wall. The filtered time domain diagram clearly shows the responses of the AD0 and AD1 channels. The time domain amplitudes of the responses of the AD0 and AD1 channels were significantly higher than those of the responses of the AD2 and AD3 channels. In the time-frequency diagram, the two wells corresponding to the AD0 and AD1 channels had a higher energy within the effective frequency range of the sand production monitoring signal and had the characteristics of sand production signals, while the time-frequency spectrum energy values of the wells corresponding to the AD2 and AD3 channels are average, and no obvious sand production signals were found. The sand production monitoring results show that the wells monitored by channel AD0 and channel AD1 were sand-producing wells, whereas the wells monitored by channel AD2 and channel AD3 did not produce sand.

In the above analysis, a high-frequency acceleration sensor was used to obtain the vibration signals of 4 wells of an offshore mining platform, and the characteristic frequency band of the sand particles was identified based on frequency domain analysis and time-frequency analysis. The background noise of the sand-carrying fluid was reduced, the sand production phenomenon of the oil well was successfully identified, and the test results of the oil field production test center were consistent. This further illustrates the feasibility of the on-site sand production monitoring method based

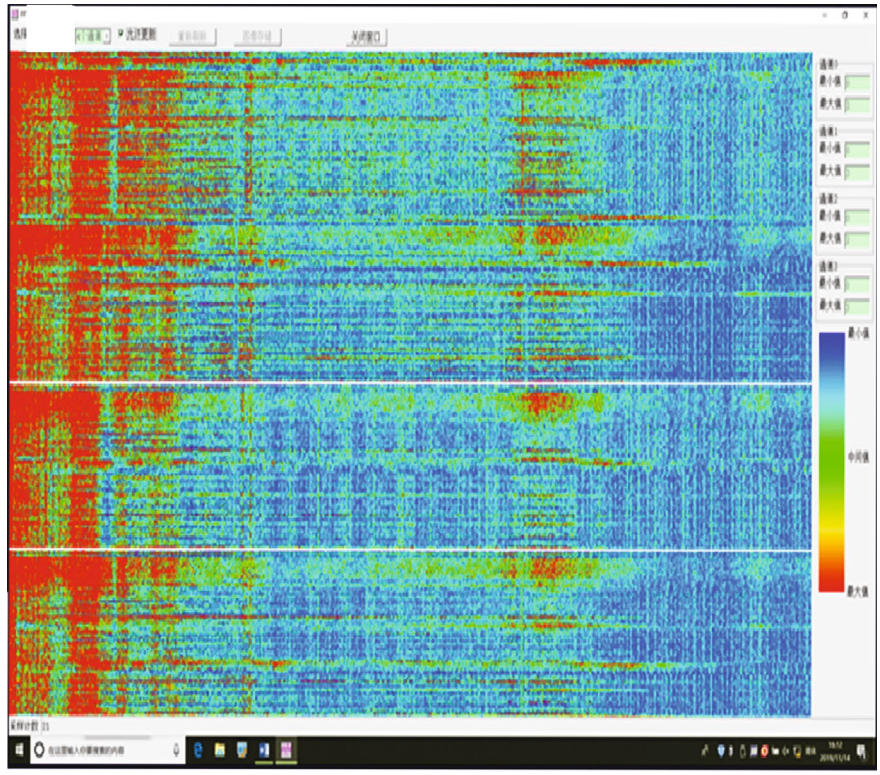

(a)

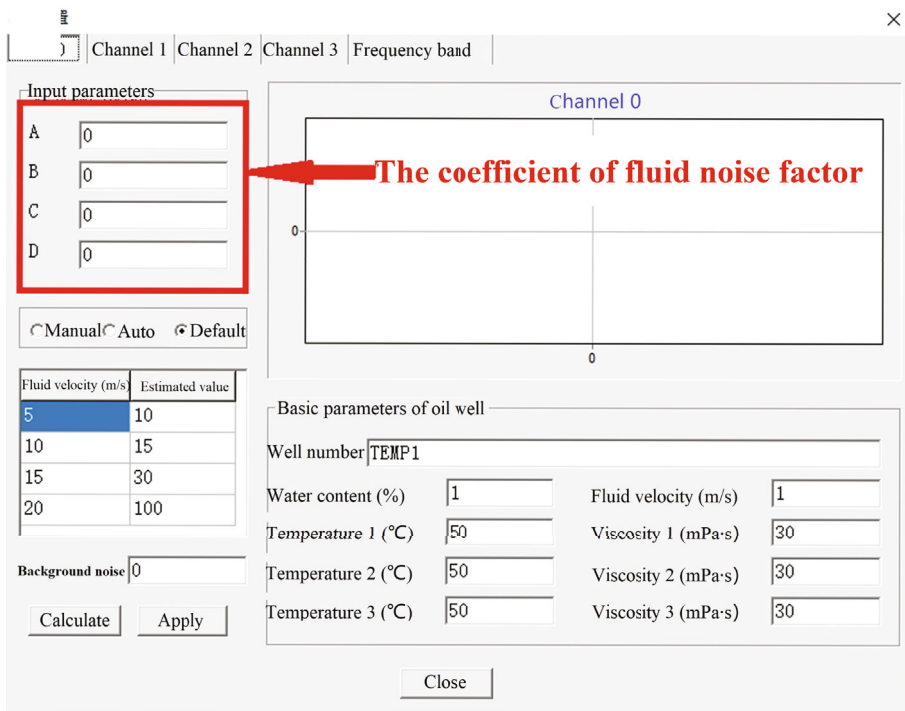

(b)

Figure 8: Sand production monitoring software system: (a) dynamic time spectrum; (b) sand monitoring module.

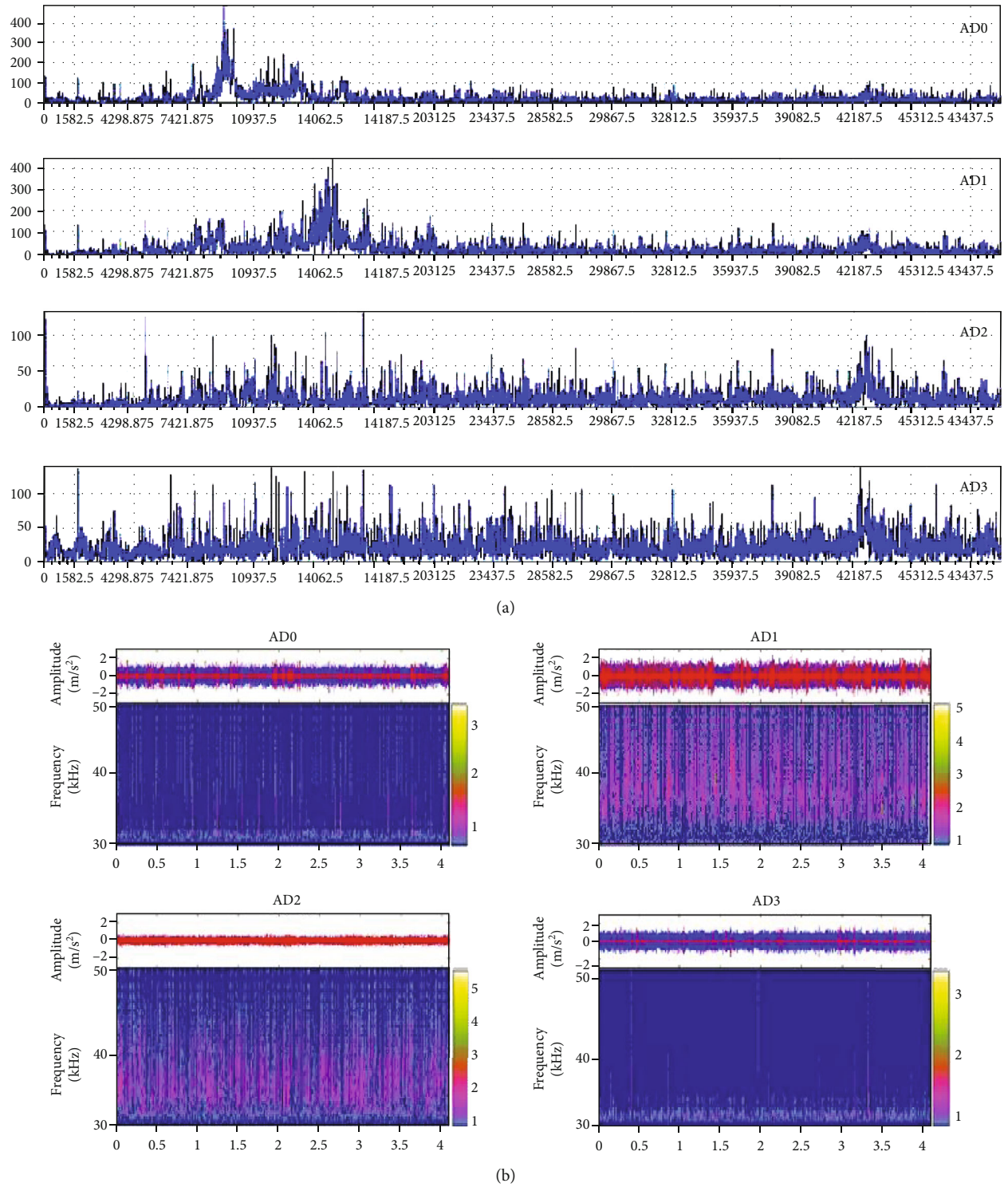

Figure 9: Analysis of the monitoring signal of sand production in the field experiment: (a) frequency domain diagram; (b) time spectrum.

on the analysis of the vibration signal of the sand-carrying fluid flow.

5. Conclusions

This paper proposed a method for monitoring the sand production of offshore oil wells based on the vibration response characteristics of the sand-carrying fluid impacting the pipe wall. Through time-frequency analysis, under different sand contents, particle sizes, and flow velocities, the frequency of the impact of the sand on the pipe wall was concentrated in the range of 30-50 kHz. Through a large number of indoor sand production monitoring and verification experiments, the vibration signal response characteristics of the sand

impacting the pipe wall were analyzed. Based on this, a real-time calculation model of sand production in offshore oil wells was constructed, and the effectiveness of the model was verified. Finally, field test research was carried out on 4 test wells of an oil production platform in the Bohai Sea, which verified the effectiveness of the method proposed in this paper.

The following conclusions were drawn:

(1) The vibration sensor was used to collect the sand vibration signal. Using STFT and digital filtering methods, the signal of the sand impacting the pipe wall and the signal of the fluid flow impacting the pipe wall were effectively distinguished in the frequency domain. The recognition ability of the weakly excited vibration signals of the sand particles in the fluid stream was enhanced. The sand vibration signal was successfully extracted from the background noise of the sand-carrying fluid

(2) By analyzing the signal characteristics of sand-carrying fluid flow with different sand contents, particle sizes, and flow velocities, the characteristic frequency band of the vibration signal of the sand impacting the pipe wall was determined to be 30-50 kHz. The characteristic law of the vibration signal excited by changes in the sand content, particle size distribution, and flow velocity was analyzed and evaluated. The time-frequency dynamic response excited by the change in the sand content increased as the sand content increased. The time-frequency dynamic response energy excited by the particles increased as the particle size increased. The time-frequency dynamic response excited by changes in the flow rate increased as the flow rate increased

(3) The sand production exhibited a good correlation with the power spectrum amplitude of the sand production monitoring signals. A sand production calculation model for oil wells was established, and a set of sand production monitoring software systems with multichannel sand production dynamic monitoring functions was compiled. Through the sand production monitoring experiment of 4 oil production wells, the reliability of the sand production monitoring method based on the vibration signal characteristics of the sand-carrying fluid flow was verified, and theoretical and technical support for the industrialization of oil well sand production monitoring was provided

Data Availability

The data used to support the findings of this study are available from the corresponding author upon request.

Conflicts of Interest

The authors declare that there are no conflicts of interest regarding the publication of this paper.

Acknowledgments

This paper was supported by the Research on Engineering Technology of Production Well Sand Management and Monitoring Equipment (No. YXKY-2018-ZY-02).

References

[1] A. Nouri, H. Vaziri, E. Kuru, and R. Islam, "A comparison of two sanding criteria in physical and numerical modeling of sand production," *Journal of Petroleum Science and Engineering*, vol. 50, no. 1, pp. 55–70, 2006.

[2] P. G. Ranjith, M. S. Perera, W. K. Perera, S. K. Choi, and E. Yasar, "Sand production during the extrusion of hydrocarbons from geological formations: a review," *Journal of Petroleum Science and Engineering*, vol. 124, pp. 72–82, 2014.

[3] S. R. Jackson, B. Gundemoni, and P. Barth, "Sand control in corrosive and erosive downhole conditions at high temperatures," in *SPE Asia Pacific Oil & Gas Conference and Exhibition*, Perth, Australia, October 2016.

[4] R. Ibarra, R. S. Mohan, and O. Shoham, "Critical sand deposition velocity in horizontal stratified flow," in *SPE International Symposium and Exhibition on Formation Damage Control, Lafayette*, Louisiana, USA, 2014.

[5] D. Dall'Acqua, M. Benucci, F. Corvaro et al., "Experimental results of pipeline dewatering through surfactant injection," *Journal of Petroleum Science and Engineering*, vol. 159, pp. 542–552, 2017.

[6] S. A. Treese, P. R. Pujadó, and D. S. J. Jones, *Handbook of Petroleum Processing*, Springer, Netherlands, 2006.

[7] T. Johnson and L. Cowie, "On-line tool for detection of solids and water in petroleum pipelines," *United states patent application publication*, 2007, US 20070189452 A1.

[8] N. A. Braaten, T. J. Blakset, and D. Morton, "Experience from topside and subsea use of the erosion based sand monitoring system," in *The SPE Annual Technical Conference and Exhibition*, pp. 147–157, Dallas, Tex, USA, October 1995.

[9] N. A. Braaten, R. Johnsen, G. Sirnes, T. Solberg, and T. Søntvedt, "A new concept for sand monitoring: sand probe based on the ER technique," in *The SPE Offshore Technology Conference*, Houston, Tex, USA, May 1992.

[10] N. Kesana, J. Throneberry, B. McLaury, S. Shirazi, and E. Rybicki, "Effect of particle size and liquid viscosity on erosion in annular and slug flow," *Journal of Energy Resources Technology*, vol. 136, no. 1, pp. 012901.1–012901.10, 2014.

[11] K. Wang, Y. Hu, Z. Wang et al., "Multi-frequency characterization of particle-wall interactions in a solid- liquid dispersion conveying pipe flow using a non-intrusive vibration detection method," *Chemical Engineering Journal*, vol. 413, p. 127526, 2021.

[12] N. C. Hii, C. K. Tan, S. J. Wilcox, and Z. S. Chong, "An investigation of the generation of Acoustic Emission from the flow of particulate solids in pipelines," *Powder Technology*, vol. 243, pp. 120–129, 2013.

[13] M. El-Alej, D. Mba, T. Yan, and S. Husin, "Investigation on sand particle impingement on steel pipe in two phase flow using acoustic emission technology," *Applied Mechanics and Materials*, vol. 315, pp. 540–544, 2013.

[14] M. Sampson, B. McLuary, and S. Shirazi, "A method for relating acoustic sand monitor output to sand rate and particle

kinetic energy," in *NACE International*, Houston, Texas, USA, 2002.

[15] M. Ibrahim and T. Haugsdal, "Optimum procedures for calibrating acoustic sand detector," in *International Petroleum Conference/SPE Gas Technology Symposium*, Alberta, Canada, 2008.

[16] G. Gao, R. Dang, A. Nouri et al., "Sand rate model and data processing method for non-intrusive ultrasonic sand monitoring in flow pipeline," *Journal of Petroleum Science and Engineering*, vol. 134, pp. 30–39, 2015.

[17] H. Zhao, H. Liu, Y. Jin, X. Dang, and W. Deng, "Feature extraction for data-driven remaining useful life prediction of rolling bearings," *IEEE Transactions on Instrumentation and Measurement*, vol. 70, pp. 1–10, 2021.

[18] K. Wang, Y. Li, Y. Hu, M. Qin, and G. Wang, "Multi-scale characterization and identification of dilute solid particles impacting walls within an oil-conveying flow with an experimental evaluation by dual vibration sensors," *Chemical Engineering Journal*, vol. 416, p. 129173, 2021.

[19] Z. Yan and R. Akira, "Wavelet multi-resolution analysis on particle dynamics in a horizontal pneumatic conveying," *Advanced Powder Technology*, vol. 29, no. 10, pp. 2404–2415, 2018.

[20] X. Shi, C. Tan, F. Dong, and Y. Murai, "Oil-gas-water three-phase flow characterization and velocity measurement based on time-frequency decomposition," *International Journal of Multiphase Flow*, vol. 111, pp. 219–231, 2019.

[21] J. Tang, C. Yan, L. Sun, Y. Li, and K. Wang, "Effect of liquid subcooling on acoustic characteristics during the condensation process of vapor bubbles in a subcooled pool," *Nuclear Engineering and Design*, vol. 293, pp. 492–502, 2015.

[22] A. Sheikhi, R. Sotudeh-Gharebagh, N. Mostoufi, and R. Zarghami, "Frequency-based characterization of liquid-solid fluidized bed hydrodynamics using the analysis of vibration signature and pressure fluctuations," *Powder Technology*, vol. 235, no. 2, pp. 787–796, 2013.

[23] M. S. Khan, G. Montes, A. Valencia, S. M. Bhatti, and N. B. Yoma, "On discriminating sizes of CFD generated bubbles with signal processing analysis," *International Journal of Heat and Mass Transfer*, vol. 89, pp. 996–1006, 2015.

[24] K. Wang, G. Liu, Y. Li et al., "Vibration and acoustic signal characteristics of solid particles carried in sand-water two-phase flows," *Powder Technology*, vol. 345, pp. 159–168, 2019.

[25] K. Wang, Y. Hu, M. Qin, G. Liu, Y. Li, and G. Wang, "A leakage particle-wall impingement based vibro-acoustic characterization of the leaked sand-gas pipe flow," *Particuology*, vol. 55, pp. 84–93, 2021.

[26] R. E. Crochiere and L. Rabiner, "Optimum FIR digital filter implementations for decimation, interpolation, and narrow-band filtering," *IEEE Transactions on Acoustics Speech and Signal Processing*, vol. 23, no. 5, pp. 444–456, 1975.

[27] P. P. Vaidyanathan, "Design of doubly-complementary IIR digital filters using a single complex allpass filter, with multirate applications," *IEEE Transactions on Circuits and Systems*, vol. 34, no. 4, pp. 378–389, 1987.